The Practical Use of the DMM Model for Life Estimation of HVDC Cables Subjected to Qualification Load Cycles

Giovanni Mazzanti, *Fellow, IEEE*

***Abstract*— A procedure for life and reliability estimation of full-size high-voltage direct current (HVDC) cables under the electrothermal transients caused by load cycles was successfully set up and applied to qualification load cycles prescribed by Cigrè TB 496 and 852. However, a gap in the procedure is that only the phenomenological electrothermal IPM-Arrhenius life model was used so far, while no physical life model was ever employed. The estimation of phenomenological life model parameters requires accelerated life test data fitting without an in-depth understanding of aging processes. Physical life models are appealing as they take degradation due to local microdefects as the main source of aging, and their parameters in principle could be derived from short-term chemical–physical measurements on small dielectric specimens. This article fills this gap by using the physical Dissado–Mazzanti–Montanari (DMM) life model for life estimation of HVDC cables under the electrothermal transients involved by qualification test load cycles. The practical difficulties in using physical models in general, and the DMM in particular, are analyzed and assessed resorting to an application relevant to pre-qualification load cycles according to TB 852.**

***Index Terms*— Extruded insulation, high-voltage direct current (HVDC) cables, life models, power system transients, qualification tests.**

I. Introduction

IN THE last two decades, research and development efforts on HVDC cable systems—particularly of the extruded type [1], [2]—turned into many HVDC cable links commissioned or planned at steadily rising voltages and powers, e.g., the ±400-kV-DC/1-GW NEMO link [3], [4] and the ±525-kV-DC/2-GW German Corridors. In such projects, sound models for estimating the life and reliability of HVDC cables are vital, as they serve for the following [5]:

1) selecting the best among novel insulation compounds from the viewpoint of endurance to applied stresses;
2) selecting stress levels and durations of load cycle voltage tests, with focus on prequalification test (PQT), extension of qualification test (EQT), and type test (TT) set by Cigrè Technical Brochure (TB) 852 [6];
3) evaluating life on duty to select design parameters of cable insulation (thickness, stress levels, and so on).

It is not easy to develop valid life and reliability models for power cable insulation, particularly if such models have to treat the typical changes in thermal and electrical stresses due to current and voltage transients on duty [5]. However, a sound procedure for life and reliability estimation of full-size HVDC cables under the electrothermal transients associated with cycles of cable load current was set up in [7] and [8]. The procedure was applied first [7], [8], [9] to the electrothermal transients caused by qualification load cycles according to Cigrè TB 496:2012 and TB 852:2021 [6]; later, the procedure was broadened to voltage transients such as long temporary overvoltages (TOVs) [10] and superimposed switching impulses (SSIs) [11].

So far, the main gaps in the life and reliability estimation procedure for HVDC cables under load cycles are two [12].

1) The procedure takes cable insulation implicitly as homogeneous, thus assuming that inhomogeneities and space charges are evenly spread all over the insulation;
2) The procedure employed only the phenomenological electrothermal IPM-Arrhenius model, while it never used any physical life model.

Let us emphasize that electrothermal (i.e., valid under constant electrical and thermal stress) life models can be classified as either physical (or microscopic) models, taking degradation due to local microdefects as the main source of aging, and phenomenological (or macroscopic or empirical) models, aiming only at a valid relationship between stresses and life [5], [12].

As for point 1 above, the author's research team is currently developing a bipolar charge transport (BCT) model for charge density and electric field calculation within the insulation thickness—taking as a reference the studies done, e.g., in [13] and [14]—to let the procedure treat nonuniform space charges.

As for point 2 above, in the procedure for full-size HVDC cables under load cycles, the usage of physical life models is much more complicated than that of the IPM-Arrhenius

Manuscript received 10 November 2023; revised 22 January 2024; accepted 8 February 2024. Date of publication 9 February 2024; date of current version 30 July 2024. This work was supported by the Italian Ministry of University and Research (Ministero dell'Università e della Ricerca, MUR).

The author is with the Department of Electrical, Electronic and Information Engineering (DEI), Alma Mater Studiorum–University of Bologna, 40136 Bologna, Italy (e-mail: giovanni.mazzanti@unibo.it).

Color versions of one or more figures in this article are available at https://doi.org/10.1109/TDEI.2024.3365047.

Digital Object Identifier 10.1109/TDEI.2024.3365047

model, as hinted at in [12] and discussed broadly in Sections III and IV. Moreover, focusing on qualification load cycles prescribed by TB 496:2012 and TB 852:2021 [6] (the main application of the procedure so far), these TBs take the IPM with life exponent $n = 10$ as the reference life model for setting voltage levels and durations of load cycle tests. For this reason, only the phenomenological IPM-Arrhenius model—that merges the IPM electrical life model with the Arrhenius thermal life model, this latter being the basis of IEC std. 60216 for thermal aging of insulation—was used in the HVDC cable life estimation procedure applied to qualification load cycles so far [7], [8], [9]. Anyway, the procedure can use any electrothermal life model valid for the insulation—including physical models.

However, the missing use of physical life models for life estimation of HVDC cables under load cycles is still a gap in the literature. Thus, as a personal commitment to the reviewers of [12], the author here fills this gap by using the Dissado–Mazzanti–Montanari (DMM) life model [15], [16] for life estimation of HVDC cable insulation under the electrothermal transients involved by qualification load cycles. The DMM model is chosen among other physical life models (see, e.g., [17], [18], [19], [20]) for two reasons: 1) it is quite flexible and fitted well accelerated life test (ALT) [21] data for small-size polymeric samples tested under dc voltage [16], [22] and 2) the author gained experience on this model during its setup and application together with the other developers.

This article is organized as follows. In Section II, the procedure for life and reliability estimation of HVDC cable insulation under the electrothermal transients due to load cycles is summarized. In Section III, the basics and the equations of the DMM model are recalled, and compared with the Arrhenius-IPM model, the DMM model is fitted to literature ALT data for a top-grade DC-XLPE, to enable life estimation of full-size DC-XLPE insulated cables through the DMM model itself. In Section IV, the procedure for life and reliability estimation of HVDC cables under electrothermal transients, using both the IPM-Arrhenius model employed so far [7], [8], [9] and the DMM model with parameters derived in Section III, is applied to prequalification load cycles according to TB 852:2021, discussing the results and the limitations exhibited by the DMM model. Section V draws some conclusions.

II. Procedure for Life and Reliability Estimation of HVDC Cables Subjected to Load Cycles

Since the main electrothermal transients in the service life of HV cables are the daily cycles of load current, a life and reliability estimation procedure for HVDC cables under such cycles was set up first in [7] and refined in [8] and [9]. The procedure consists of six steps or "blocks" [12], see the block diagram of Fig. 1. Details, found in [7], [8], [9], and [12], are omitted here for brevity, with two exceptions for the sake of clarity.

First, focusing on block 3 in Fig. 1, let us note that the calculation of transient electric field $E(r, t)$ in cable insulation is done either in a rigorous way (exact procedure [8], left branch in block 3), i.e., solving Maxwell's equations, or in an approximate way (approximated procedure [7], right branch in block 3) through Eoll's formula [23], often used in the technical scientific literature for a first guess of dc field [24], [25].

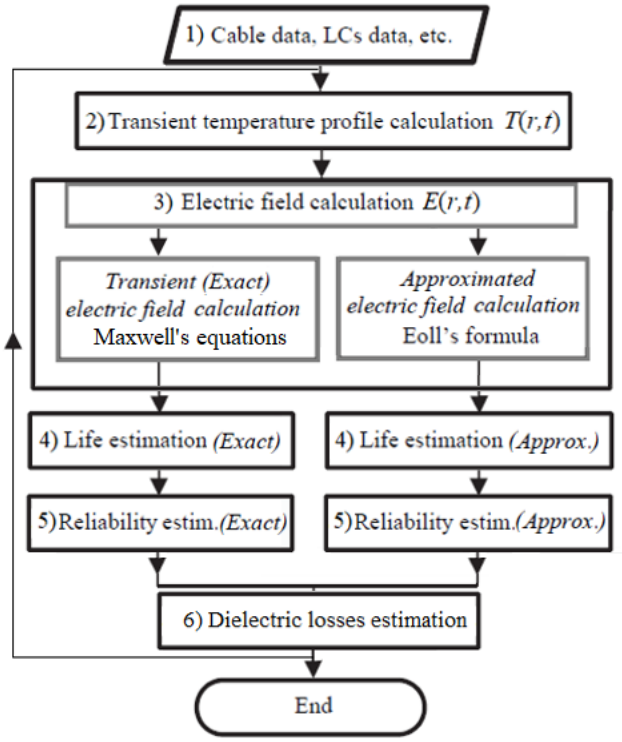

Fig. 1. Block diagram of the procedure for life and reliability estimation of HVDC cables subjected to load cycles.

Second, focusing on block 4 in Fig. 1, let us note that the estimation of HVDC cable insulation life under load cycles, L^*_{cycle}—namely the life of the insulation at the most stressed radius r^* yielding the minimum number of cycles-to-failure, K^*_{cycle}—is accomplished via the following set of equations:

$$dLF(r,t) = dt/L[E(r,t), T(r,t)] \tag{1}$$

$$LF_{\text{cycle}}(r) = \int_0^{t_d} dLF(r,t) \tag{2}$$

$$K_{\text{cycle}}(r) = 1/LF_{\text{cycle}}(r) \tag{3}$$

$$L_{\text{cycle}}(r) = t_d \times K_{\text{cycle}}(r) \tag{4}$$

$$L^*_{\text{cycle}} = \min\left\{L_{\text{cycle}}(r), r \in [r_i, r_o]\right\} = t_d \times K^*_{\text{cycle}} \tag{5}$$

where $dLF(r, t)$ is the life fraction lost by the insulation within each time interval dt wherein $E(r, t)$ and $T(r, t)$ can be taken as constant; $L[E(r, t), T(r, t)]$ is the insulation life at $E(r, t)$ and $T(r, t)$; $LF_{\text{cycle}}(r)$ is the fraction of life lost during each cycle of duration t_d at each radius r; $K_{\text{cycle}}(r)$ is the number of cycles-to-failure, derived from (2) by setting to 1 the sum of all $LF_{\text{cycle}}(r)$ at failure (Miner's law of cumulated damage); and $L_{\text{cycle}}(r)$ is the life under load cycles at insulation radius r.

Let us emphasize that in (1), cable insulation life $L(E, T)$ at field $E = E(r, t)$ and temperature $T = T(r, t)$—assumed as constant between t and $t + dt$—can be obtained from any life model holding for HVDC cable insulation under constant electrical and thermal stress, i.e., from any valid

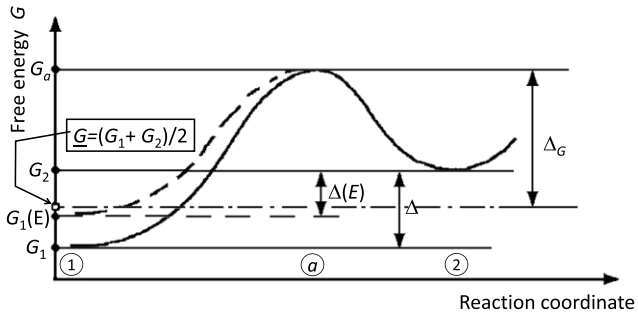

Fig. 2. Free energy diagram in the absence (solid line) and in the presence (dashed line) of electric field.

electrothermal life model. As pointed out in Section I, so far [7], [8], [9], [17], only the phenomenological electrothermal IPM-Arrhenius life model was used in the procedure here described for the estimation of full-size HVDC cable life under qualification load cycles [6] since the IPM and the Arrhenius life models are, respectively, the reference electrical and thermal life models of International Standards for HVDC cable insulation. The goal here is to use also the physical electrothermal DMM model for full-size HVDC cable life estimation under qualification load cycles.

III. DMM Model for Full-Size HVDC Cables

A. DMM Model in Summary

The DMM life model, conceived for polymeric extruded insulation, is a physical electrothermal life model with a thermodynamic background. Thermodynamic models treat the aging under temperature and voltage (electrothermal aging) of electrical insulation as a thermally activated process [5], [26], where the following conditions hold (see Fig. 2).

1) A dielectric turns from unaged or "reactant" state 1 (= free energy G_1) to aged or "degraded" state 2 (= free energy G_2) as an activation free energy barrier Δ_G is exceeded.
2) Electric field E raises G_1 to $G_1(E)$ through the local storage of electromechanical energy, thus reducing the free energy barrier via a field-dependent barrier-lowering term.

The DMM model is maybe the first physical life model where space charges stored in the insulation play a key role in the electrothermal aging and failure of polymeric dielectrics for dc cables [15], [16]. Its main hypotheses are as follows.

I) The polymeric insulation of HVDC cables is affected by spherical micro- or nano-voids of radius r_V, capable of trapping an amount $q_C = C_q\ E^{bq}$ of the space charge injected by the electrodes, where C_q and b_q are parameters related to the space-charge accumulation features of the dielectric [16], [27]. At space-charge storage centers, the space-charge Poissonian field overwhelms the dc voltage field.
II) Each center degrades N_m microstructural units, referred to as "moieties"—e.g., inter-/intra-chain bonds and cross-linking bonds in cross-linked polymers—encompassed within a shell of thickness λ at the void boundary.
III) Aging stems from a competition between a forward reaction from state 1 to state 2, and a backward reaction from state 2 to state 1 (see Fig. 2), both partly reversible. The conversion of a moiety from state 1 to state 2 introduces a fixed strain δ_S, called an elemental strain, which is typical of the polymeric dielectric.
IV) Breakdown is started locally as soon as the fraction of degraded moieties, A, exceeds a critical value, A^*, which depends on the dielectric. This starts an electrical tree that bridges the electrodes quite soon. Hence, insulation life (= time-to-failure) practically coincides with the time to electrical treeing inception.

From the above assumptions, the DMM model yields electrothermal life $L(E, T)$ according to the following set of equations:

$$L(E,T) = \frac{h_P}{2k_BT}\exp\left(\frac{\Delta_H/k_B - C'E^{2b_q}/2}{T} - \frac{\Delta_S}{k_B}\right) \times \ln\left[\frac{A_{eq}(E)}{A_{eq}(E)-A^*}\right]\left[\cosh\left(\frac{\Delta/k_B - C'E^{2b_q}}{2T}\right)\right]^{-1} \tag{6}$$

$$A_{eq}(E) = 1/\left\{1+\exp\left[\left(\Delta/k_B - C'E^{2b_q}\right)/T\right]\right\} \tag{7}$$

$$C' = \left(B_q\alpha_E\delta_S\lambda C_q^2\right)/\left(16\pi\varepsilon^2 r_V^2 N_m k_B\right) \tag{8}$$

$$E_{th}(T) = \left\{\left[\Delta/k_B - T\ln\left(\left(1-A^*\right)/A^*\right)\right]/C'\right\}^{1/(2b_q)} \tag{9}$$

$$\delta_S = \sqrt{\frac{2k_BTN_m}{KB_q\exp\left[\Delta/(k_BT)\right]N_C}}\,\frac{1+\exp\left[\Delta/(k_BT)\right]}{4\pi r_0^2\lambda} \tag{10}$$

where [15], [16]: k_B is Boltzmann's constant; h_P is the Planck constant; $\Delta_G = G_a - (G_1+G_2)/2$ is the activation free energy per moiety without electric field, split into $\Delta_H = H_a - (H_1 + H_2)/2$ is the activation enthalpy per moiety and $\Delta_S = S_a - (S_1+S_2)/2$ is the activation entropy per moiety; $\Delta = G_2 - G_1$ without electric field, independent of temperature; $A_{eq}(E)$ is the value of A at the equilibrium between forward and backward reaction; C' is a constant typical of the dielectric, being B_q the proportionality constant between stored electromechanical energy per moiety and its contribution to the free energy barrier of degradation; α_E is the electrostriction coefficient; δ_S is the elemental strain; N_C is the cavity density within the insulation; K is the bulk modulus, playing here the same role as Young's modulus in macroscopic insulation; and $E_{th}(T)$ is the electrical threshold (function of T), i.e., a field level below which electrical aging stops and life tends to infinity, in agreement with the threshold for space-charge accumulation guessed in the range 10–20 kV/mm at room temperature for dc polymeric insulation [27], [28].

Some parameters of the DMM model can be derived from short-term physical measurements on small dielectric samples.

- As hinted at point I above, short-term measurements of space-charge trapped within unaged insulation samples—e.g., carried out by means of the pulsed electro-acoustic (PEA) technique—fit quite well a power law $q_C = C_q\ E^{bq}$, with b_q in the range 0.3–0.7, and hence, such measurements could provide parameter b_q [5], [15], [16], [27], [28].

- E_{th} can be guessed via space charge, electroluminescence, and conduction current measurements on unaged samples [27]; thermal threshold T_{th} (the thermal analog of E_{th}) can be estimated from chemico-physical tests on the dielectric (e.g., oxidative stability measurements [29]). Then, being $T_{\text{th}} = (\Delta/k_B)/[\ln(1-A^*)/A^*]$ [28] and E_{th} given by (9), one gets two more relationships between Δ, A^*, and C'.
- $\Delta_G = \Delta_H - T\Delta_S$ can be derived from oxidative stability [e.g., oxidation induction time (OIT)] measurements [17], [18], [29], [30], thus yielding a relationship between Δ_H and Δ_S.

The DMM model performed well also as a phenomenological model for ALT data relevant to different dielectrics tested under dc and ac voltage [15], [16], [31], among which unluckily only one is of interest to this article, i.e., the very good fitting of ALT data for 0.15-mm-thick DC-XLPE press-molded plaques subjected to dc voltage at 20 °C [16]. Regrettably, this single test temperature did not enable to derive a complete dataset of DMM model parameters, as discussed here. In addition, the ALT data in [16] are fairly old: more recent data are needed to update the DMM model parameters to state-of-the-art HVDC cable insulation, as shown hereafter in Section III-C.

B. DMM Model Versus the Arrhenius-IPM Model

As pointed out above, so far, only the phenomenological IPM-Arrhenius model was used in (1) (block 4 of Fig. 1) to express cable insulation life $L(E, T)$ in the procedure for full-size HVDC cables subjected to qualification load cycles [7], [8], [9], [12]. This model—obtained merging the IPM electrical model with the Arrhenius thermal model [5, Ch. 6]—is one of the most popular electrothermal life models in the literature on cable insulation and can be written as [7], [8], [9], [12]

$$L(E,T) = L_D\left[E/E_D\right]^{-(n_D - b_{ET}T_d)}\left[E_D/E_0\right]^{b_{ET}T_d} e^{-BT_d} \quad (11)$$

where T_D, E_D, and L_D are design temperature, field, and life (at design failure probability P_D), respectively, of full-size HVDC cable; $T_d = 1/T_D - 1/T$; n_D is the life exponent [or voltage endurance coefficient (VEC)] at temperature T_D; E_0 is the reference electric field below which electrical aging ceases; and b_{ET} is the synergism parameter between electrical and thermal stress [7], [8], [9], [12].

As hinted at above, and also seen from (11), the IPM-Arrhenius is the most practical and viable electrothermal life model for full-size HVDC cables for the following reasons.

1) The IPM and the Arrhenius life models are, respectively, the reference electrical and thermal models of International Standards for HVDC cable insulation [5], [6].
2) The IPM and the Arrhenius life models are simple and flexible, so as to fit satisfactorily ALT data for various HVDC cable insulating compounds tested with different fields, temperatures, and test cells. Such flexibility is transferred to their combination, namely, the IPM-Arrhenius electrothermal life model [5], [12].
3) The IPM-Arrhenius life model can be used to establish the voltage level of dedicated load cycle tests at constant voltage, provided that design life L_D, design VEC n_D, and number of cycles N_T are fixed. As the most noteworthy example for HVDC extruded cables, the voltage level $U_{\text{PQT}} = 1.45U_0$ of PQT 24 h-load cycles is derived in [6] by setting $L_D = 40$ y, $n_D = 10$, $N_{\text{PQT}} = 360$, as well as the voltage level $U_{\text{TT}} = 1.85U_0$ of the TT 24 h-load cycles by setting $L_D = 40$ y, $n_D = 10$, and $N_{\text{TT}} = 30$. This derivation is approximated, as it neglects thermal aging during the load cycles; this makes qualification load cycle tests less challenging than expected, see [7], [8], [9] and hereafter in Section IV.
4) The IPM-Arrhenius model features five parameters—i.e., n_D, B, b_{ET}, E_D, and E_0, since T_D and L_D (and P_D) are known and fixed from design specifications—whereas the DMM model features six parameters, i.e., Δ_H, Δ_S, Δ, C', b_q, and A^*, of which C' is a "phenomenological-like" parameter as it depends on several quantities not easily estimated from chemical–physical measurements on the dielectric, i.e., B_q, α_E, δ_S, λ, C_q, ε, r_V, and N_m. Hence, the overall estimation of the six parameters of the DMM model is more complex and uncertain than the already nontrivial evaluation of the five parameters of the IPM-Arrhenius model.

Conversely, the use of the DMM model for full-size HVDC cables is much more cumbersome than that of the IPM-Arrhenius, as readily seen when comparing (6)–(10) with (11), considering also that in (11), a direct reference can be made to the design life L_D, field E_D, and temperature T_D of the full-size cable, which is missing in (6)–(10).

C. Estimation of DMM Model Parameters for Full-Size HVDC Extruded Cables

To fill the gap and enable the use of the physical DMM life model for life and reliability estimation of HVDC cables under qualification load cycles, an adequate set of DMM model parameters for full-size HVDC extruded cables needs to be found. As it can be agreed, "adequate" means that such set of DMM model parameters should match the following requirements.

i) Be updated to state-of-the-art HVDC cable insulation.
ii) Be complete of all parameters, i.e., Δ_H, Δ_S, Δ, C', b_q, A^*.
iii) Be adapted to full-size cables, if it is derived (as usual) from small specimens tested in the laboratory.

As hinted at above, finding such adequate set is hard. In fact, it is not trivial to find detailed and exhaustive data of chemical–physical measurements or electrothermal ALTs for state-of-the-art HVDC extruded insulation compounds from which an adequate set of DMM model parameters can be derived. Indeed, these data are highly sensitive and known to manufacturers only, because of the great commercial and strategic value of HVDC extruded cable systems nowadays. Solely, one set of DMM model parameters was proposed so far for HVDC polymeric cable insulation, obtained from the abovementioned fitting of ALT data for 0.15-mm-thick DC-XLPE plaques tested under dc voltage at room temperature reported in [16]. This set of DMM model parameters,

TABLE I
PROSPECTIVE DMM MODEL PARAMETERS FOR HVDC CABLES

Parameter [Units]	Values after [16]	Derived here from the ALTs after [32],[33]
Δ_H [J]	$\Delta_G(20°C)=2.1\ 10^{-19}$	$1.564\ 10^{-19}$
Δ_S [J]		$-3.75\ 10^{-22}$
Δ [J]	$3.4\ 10^{-21}$	$4.03\ 10^{-21}$
C' [K(MV/m)$^{-2bq}$]	$8\ 10^{-4}$	0.1833
b_q [n.d.]	1.438	1
A^* [n.d.]	0.305	0.305

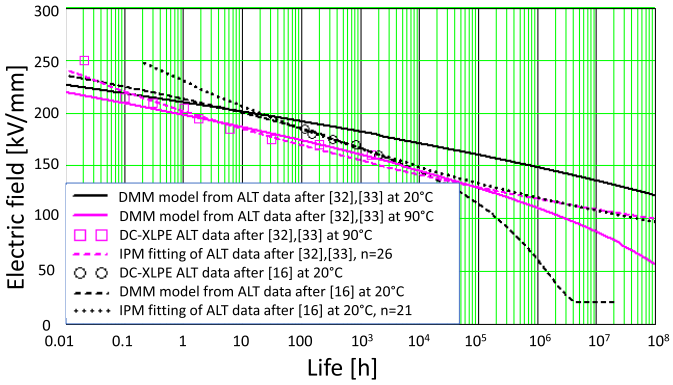

Fig. 3. DMM model life estimates at 20 °C (black solid line) and 90 °C (magenta solid line) with parameters from fitting DC-XLPE ALT data at 90 °C after [32], [33] (boxes, Courtesy Sumitomo); the fitting of the same data via the IPM with $n = 26$ is also reported (magenta dashed line). DC-XLPE ALT data at 20 °C after [16] (circles) and their fitting via DMM model with parameters after [16] (black dashed line) and IPM (black dotted line) are shown.

listed in Table I, second-to-last column, under the heading "values after [16]," is not adequate as it violates all three above requirements i)–iii). Indeed, the following conditions hold.

1) It is fairly old, as it dates back to 2001 [16], although the same dataset was used recently in [22].
2) It is incomplete since the ALT data in [16] are relevant to room temperature only and their phenomenological fitting provided just the activation free-energy $\Delta_G(20\ °C) = 2.1 \times 10^{-19}$ J (a value quoted also in [18]), but without splitting $\Delta_G = \Delta_H - T\Delta_S$ into enthalpy Δ_H and entropy Δ_S.
3) It is focused on small specimens rather than on full-size cables, as it comes from very small and thin flat samples.

For these reasons, the DMM model parameter set reported in Table I, last column, under the heading "from the ALTs after [32], [33]," is taken here to use the physical DMM life model for life estimation of HVDC cables under load cycles. Such set is in fact obtained here fitting the ALT data after [32]—reported also in [33] and relevant to a more recent top-grade DC-XLPE tested under dc voltage at 90 °C—by means of the Levenberg–Marquardt optimization algorithm, with the parameter set after [16] as initial guess. The values of Δ_H and Δ_S derived here, in fair agreement with values reported, e.g., in [34], lead to values of Δ_G ranging from $\Delta_G(20\ °C) = 2.6 \times 10^{-19}$ J to $\Delta_G(100\ °C) = 2.9 \times 10^{-19}$ J. For XLPE, such variation of Δ_G in the range 20 °C−100 °C is in agreement with [16], [30], and [31]; the single values are ≈30% higher than those in [16], [18], [30], and [31] but are consistent with values found, e.g., in [17] for XLPE, or in [34] for polymers with a large cohesion energy. However, it can be argued that the XLPEs considered in [16], [18], [30], and [31] are fairly older than the DC-XLPE after [32] and [33], still regarded in recent years 2019–2020 as valid for reproducing the behavior of a top-grade DC-XLPE used in milestone HVDC cable link projects [3], [4]. Moreover, $\Delta_G = \Delta_H - T\Delta_S$ increases both with temperature and with the degree of additives (e.g., water tree retardants) [17], as well as with the cohesion energy of the polymer matrix [34], proportional to its thermomechanical endurance. In fact, the higher values of $\Delta_G(20\ °C)$ and $\Delta_G(100\ °C)$ found here might be associated with the inorganic nanofiller and the better thermal endurance of the DC-XLPE after [32], [33], which has a rated temperature of 90 °C: this is well above the 70 °C of most state-of-the-art DC-XLPEs [2].

The novel dataset in the last column in Table I is consistent with the following values of microstructural parameters in the DMM model: $r_0 = 10$ nm, $\lambda = 1$ nm, $N_m = 1$, $N_c \approx 10^{18}$ m^{-3}, $K = 2.2 \times 10^9$ N/m^2, $B_q = 1$, and $\delta_S = 3.41$. These values are all close to those from the fitting of data after [16], except for N_c, which is one order of magnitude lower, as reasonable in updated DC-XLPE with reduced space-charge storage; and $\delta_S \approx 3$ times greater, leading definitively to irreversible structural deformation [16]. However, they are all acceptable in terms of what is known about charge storage center size expected to be effective in aging.

Fig. 3 shows the life estimates obtained here at 20 °C (black solid line) and at 90 °C (magenta solid line) by means of the DMM model (6)–(10) with the parameters from the ALTs after [32] (magenta boxes): these are the parameters reported in the last column of Table I; the DMM model at 90 °C fits such data after [32] almost as well as the IPM fitting of the same data with life exponent $n = 26$ (magenta dashed line, see Fig. 4 of [32]). The figure also shows the DC-XLPE flat specimen ALT data at 20 °C after [16] (black circles), fitted via the DMM model with parameter values after [16] listed in the second-to-last column of Table I (black dashed line). This fitting is very good, too, but—apart from very short times and very high fields—at 20 °C, the DMM model with parameters after [16] provides much shorter lives than the DMM model with parameters from the ALTs after [32], [33]; in addition, as the field tends to qualification and design levels, the parameter set after [16] provides shorter lives at 20 °C than the parameter set from the ALTs after [32] and [33] at 90 °C: this confirms that the latter parameter set reproduces better the improved performance of state-of-the-art DC-XLPE. Finally, but not least, Fig. 3 also shows the IPM fitting on DC-XLPE ALT data at 20 °C after [16] (black dotted line), with correlation coefficient $r = 0.984$ and $n = 21$; thus, the data after [16] align well in the $\log E$–$\log L$ plot.

The DMM model parameter set in the last column in Table I is "adequate" as it matches all above requirements i)–iii).

i) It is updated to state-of-the-art HVDC cable insulation, as it comes from ALT data appearing for the 1st time in 2013 [32] and later in 2014–2020 as referred to a top-grade DC-XLPE for HVDC cable links [3], [4], [33].

ii) It is complete, as it splits Δ_G into Δ_H and Δ_S contributions.
iii) It is prone to be extrapolated to full-size cables.

As for this last requirement, a few different strategies are available to adapt the DMM model parameter values obtained from small flat specimen ALT data after [32] and [33] to full-size cables tested according to TB 852 as follows.

A first strategy—developed in [31]—is to explain the volume dependence of DMM life model parameters in full-size cables through a "scaled-up" shell approach, based on the failure probability of multiple coaxial thin shells constituting the insulation, each with constant values of E and T, and scaled-up to the whole cable insulation volume. The methodology was used in [31] to fit MVAC cable lifetimes versus applied voltage starting from the DMM life model parameters relevant to ac minicables. This strategy requires multiple failure times at multiple field levels, available in [31] for MVAC cables (i.e., cables of smaller size than HV cables and working under ac rather than dc voltage). As to the best knowledge of the author, no datasets of cable lifetimes versus dc voltage relevant to HVDC full-size cables can be found in the literature, also because such datasets—if any—are sensitive data known to manufacturers only, as emphasized above. For this reason, the nontrivial approach after [31] is unpractical for full-size HVDC cables.

Another strategy—developed in [22]—is to simulate directly on a 2-D (or 3-D) grid in a proper electrode arrangement the elementary parts of the "large" insulation, which are "broken" (i.e., turned from insulating to conducting) like elementary bonds as aging goes on. In [22], the aging of a "large" sample was evaluated under constant stress in all elemental bonds via the DMM kinetic equations by assigning them randomly selected model parameter values from thin film distributions obtained through the parameter dataset in the second-to-last column in Table I. Such a strategy seems more appropriate for a local analysis of susceptibility of weaker or defective regions than for extrapolating the behavior of fairly homogeneous, well designed, and manufactured state-of-the-art HVDC cables that are being qualified and installed nowadays worldwide at increasing levels of voltage [2], [6], [11].

The strategy followed here, deemed as the most appropriate for full-size HVDC cables, is based on the "power cable enlargement law" [24], [25], [35], often applied to extrapolate the results obtained from small cables tested in the laboratory to HV cables. As can be shown from [35], under the generalized Weibull distribution hypothesis, this strategy provides electrothermal life $L_2(E, T)$ of full-size cable insulation—with enlarged length l_2, inner radius r_{i2} and outer radius r_{o2}—from electrothermal life $L_1(E, T)$ of smaller cable insulation—with length $l_1 < l_2$, inner insulation radius $r_{i1} < r_{i2}$ and outer insulation radius $r_{o1} < r_{o2}$

$$L_2(E,T) = L_1(E,T) / \left[(l_2/l_1)^{1/\beta_E} (r_{i2}/r_{i1})^{2/\beta_E} H_{12} \right]^{\beta_E/\beta_t} \quad (12)$$

$$H_{12} = \left[\frac{2-\eta_1}{2-\eta_2} \frac{(r_{o2}/r_{i2})^{2-\eta_2} - 1}{(r_{o1}/r_{i1})^{2-\eta_1} - 1} \right]^{1/\beta_E} \quad (13)$$

where $\eta_j = (1-\delta_j)\beta_E$; δ_j is the field inversion coefficient [5], [25], $j = 1, 2$; β_E is the shape parameter of the Weibull probability distribution function (pdf) of breakdown fields/voltages; and β_t is the shape parameter of Weibull pdf of failure times [25], [35]. Generally, $\beta_E \geq 10$ for HVDC cable dielectrics, so typically, $H_{12} \approx 1$ [24], [25]; thus, cable length plays a main role in the enlargement [24].

From (12), the so-called enlarged electrothermal reliability model was derived in [35] to link the test failure probability P_T (typically 50% or 63.2%) of ALT failure times obtained in the laboratory from tests on small-size specimens (e.g., the squares and circles in Fig. 3) to the design failure probability P_D (or reliability R_D) of the full-size cable. The enlarged electrothermal reliability model is written here in a more general form than in [35]—holding whichever phenomenological or physical life model valid for the insulation is used to express $L_1(E, T)$ in (12)—i.e.,

$$t_{D,2}(E,T) = \frac{t_{T,1}(E,T)}{DP} \quad (14)$$

$$DP = \left\{ (l_2/l_1)(r_{i2}/r_{i1})^2 H_{12}^{\beta_E} \left[\ln(1-P_T)/\ln(1-P_D) \right] \right\}^{1/\beta_t}. \quad (15)$$

Relationship (14) is complicated, but powerful, as it explains $t_{D,2}(E, T)$ = life of full-size HVDC cable insulation at design failure probability P_D (i.e., the 100-P_D^{th} percentile of full-size HVDC cable failure time) as a function of $t_{T,1}(E, T)$ = 100-P_T^{th} percentile of small-size specimen failure times, estimated at electric field E and temperature T via the life model used to fit ALT failure times obtained in the lab. The name of (14) is "enlarged electrothermal reliability model" as it also yields reliability $R = 1-P$ [5], [35].

After computing the dimensional-probabilistic factor DP, $t_{D,2}(E, T)$ can be inserted for $L(E, T)$ in (1), block 4 of Fig. 1, to estimate HVDC cable insulation life at design failure probability P_D in the presence of the electrothermal stress caused by load cycles. In Section IV, $t_{D,2}(E, T)$ is expressed.

1) Directly via the phenomenological IPM-Arrhenius life model (11), as already done in [7], [8], and [9]. In this case, DP is not needed, as the IPM-Arrhenius life model (11) already contains T_D, E_D, and $L_D(P_D)$ for the full-size cable.
2) By replacing $t_{T,1}(E, T)$ in (14) with the physical DMM life model (6)–(10), for the first time here in the literature.

IV. Application of the DMM Model for Full-Size HVDC Cable Life Estimation Under Load Cycles

The procedure described in Section II is applied here to evaluate the PQT life (i.e., the life under PQT load cycles for HVDC extruded cables qualified according to [6]) of the same cable already treated in [7] and [8], i.e., a 320-kV-DC VSC XLPE-insulated land cable, whose main dielectric and design parameters appear in Table II. Transient temperature and field profiles for this cable are omitted here for brevity, as they already appeared in [7] and [8]. The novelty here, as pointed out above, is that—beside the phenomenological IPM-Arrhenius model employed so far [7], [8]—the physical

DMM life model (6)–(10) is used, with the parameter set listed in Table I, last column. Thus, $L(E, T)$ in (1), block 4 of Fig. 1, is expressed.

1) As in [7] and [8] directly via the phenomenological IPM-Arrhenius life model (11), with the same values of parameters in (11) as in [7] and [8] for the sake of comparison and consistency, i.e., $L_D = 40$ y, $P_D = 1\%$ ($R_D = 99\%$, see also Table II), $n_D = 10$, $B = 12\,430$ K, and $b_{\mathrm{ET}} = 0$.
2) Via $t_{D,2}(E, T)$ of (14), by replacing $t_{T,1}(E, T)$ with the physical DMM life model (6)–(10) with the parameter values reported in the second column of Table I.

In case 2, the use of the DMM model is more troublesome than the IPM-Arrhenius model. Indeed, full-size cable design field E_D, temperature T_D, and life L_D (at design probability P_D) appear directly in (11); on the contrary, also the values of l_2, r_{i2}, r_{o2}, l_1, r_{i1}, r_{o1}, P_T, β_E, and β_t are needed in (14) and (15) to extrapolate the values of DMM model parameters—obtained from ALT data on small-size specimens after [32], [33]—to the full-size HVDC cable. While the values of l_2, r_{i2}, and r_{o2} for the treated cable stem from Table I, the values of l_1, r_{i1}, r_{o1}, P_T, β_E, and β_t are missing in [32] and [33]. A helpful observation is that the missing values should yield a value of $t_{D,2}(E_D, T_D) = 40$ years in (14)—with $t_{T,1}(E, T)$ given by the DMM model (6)–(10)—equal to $L_D = 40$ years at T_D, E_D, and P_D used in the IPM-Arrhenius model (11) and reported in Table II. This agreement is highly desirable since the following conditions hold.

1) It ensures full consistency in the comparison between the PQT life estimates achieved here with the DMM model and those obtained in [7] and [8] with the IPM-Arrhenius.
2) It is meaningful in practice, as $L_D = 40$ years at T_D, E_D, and P_D agrees with the design life reported in [6], being thus consistent with the good performance during PQT and in service of state-of-the-art DC-XLPE insulated cables—whose performance might even be better, see the far higher value $n = 26$ of the VEC in Fig. 1 versus $n_D = 10$ used in [6] and thus in the IPM-Arrhenius model.

A careful analysis reveals that a value of $t_{D,2}(E_D, T_D) = L_D = 40$ years is compatible with the following reasonable choices of missing quantities: $P_T = 0.50$ (median failure probability), a common choice for laboratory ALTs on small-size specimens; "model A" cables (suggested for R&D tests by Cigrè TB 636) chosen as the "small cable 1" to be enlarged to full-size cable 2 in (14), taking a reduced length l_1 and thickness $r_{o1} - r_{i1}$ compared to those of real model A cables ($l_1 = 400$ mm, $r_{i1} = 1.4$ mm, and $r_{o1} = 2.9$ mm) to account for the smaller area and thickness (but subjected to uniform field) of flat specimens tested in [32] and [33]; and $\beta_t \approx 1.6$, indicating a mild and reasonable aging level.

Fig. 4 shows the log–log plot of electric field (y-axis) versus treated cable life (x-axis) estimated via: the DMM model with outer insulation temperature $T(r_{o2})$ equal to $T_D = 55.9$ °C (blue solid line)—corresponding to rated conductor temperature $T_{\mathrm{cond,max}} = 70$ °C according to steady-state thermal calculations—and 70 °C (red solid line) and the IPM-Arrhenius model with $T(r_{o2}) = T_D = 55.9$ °C (blue dashed line) and 70 °C (red dashed line). Design temperature T_D and design field E_D at rated voltage U_0 are set at the outer insulation, as this critical interface between cable and accessories requires a careful stress control; T_D and E_D provide design life $L_D = 40$ y at failure probability $P_D = 1\%$ (see Table II): "design coordinates" L_D and E_D are highlighted by a blue diamond point in Fig. 4. This figure includes the DC-XLPE flat specimen data at 90 °C after [32] and [33] (magenta boxes) and the relevant fit via the IPM with $n = 26$ (magenta dashed line) from Fig. 3 to compare cable versus small specimen data. In Fig. 4, the electric field at outer insulation under PQT voltage $U_{\mathrm{PQT}} = 1.45U_0$ and TT voltage $U_{\mathrm{TT}} = 1.85U_0$ are highlighted via two horizontal dashed-dotted lines (black and brown, respectively) to compare the life forecast by the DMM and the IPM-Arrhenius model at qualification fields: at U_{PQT} and U_{TT}, the DMM model provides a life much greater than the IPM-Arrhenius model; hence, the former is more optimistic at qualification fields. For this reason, it is expected that—under load cycles—PQT life and TT life (this latter omitted here for the sake of brevity) will be much greater for the DMM model than for the IPM-Arrhenius.

TABLE II
MAIN DESIGN PARAMETERS OF THE TREATED CABLE [7], [8]

Parameter		Value
Rated DC voltage / power / converter		320 kV /1105 MW / VSC
Conductor material /Rated temperature /X-section		Cu / 70°C / 1600 mm^2
Insulation material / thickness		DC-XLPE /17.9 mm
Design life L_D / failure probabil. P_D / reliability R_D		40 years / 1 %/ 99%
Laying environment type / temperature		Soil / 20 °C
Rated conductor temperature $T_{cond,max}$		70°C
Design temperature of outer insulation, T_D		55.9°C
PQT cable loop length l_1		100 m
Parameters of electrical conductivity	σ_0 (σ at 0°C and 0 kV/mm) [S/m]	10^{-16}
	Temperature coefficient α [1/°C]	0.084
	Field coefficient b [mm/kV]	0.0645

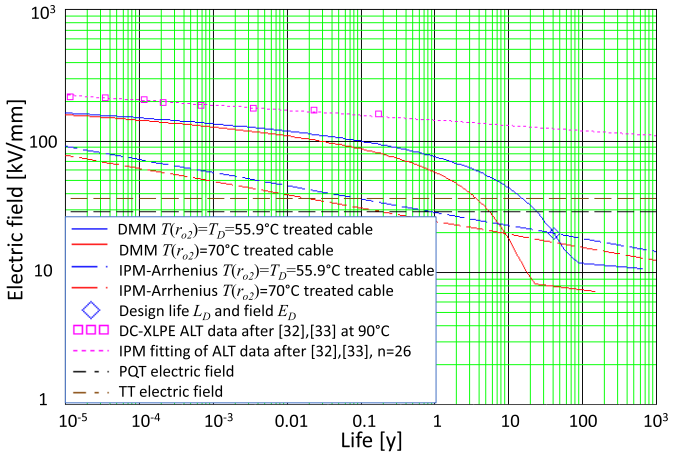

Fig. 4. For the treated cable, log–log plot of electric field versus life estimated with: DMM model at $T_D = 55.9$ °C (blue solid line) and 70 °C (red solid line); IPM-Arrhenius model at $T_D = 55.9$ °C (blue dashed line) and 70 °C (red dashed line). Blue diamond = design point $L_D(E_D, T_D)$ at outer insulation. Magenta boxes = DC-XLPE flat specimen data at 90 °C after [32] and [33] and the relevant fit via the IPM with $n = 26$ (magenta dashed line). Dashed-dotted black line: PQT field. Dashed-dotted brown line: TT field.

TABLE III
INSULATION LIFE $L_{CYCLE}(r)$ WITH RIGOROUS (EXACT) AND APPROXIMATE FIELD PROFILES AT INNER AND OUTER INSULATION OF THE TREATED CABLE. PQT LIFE L^*_{CYCLE} IS DENOTED BY A GRAY-SHADED CELL

	$L_{cycle}(r)$ [y]				$R_{cycle}=L_{cycle,DMM}(r)/L_{cycle,IPM\text{-}Arr.}(r)$	
Models →	IPM-Arrhenius [8]		DMM			
radius ↓	Exact field	Approx. field	Exact field	Approx. field	Exact field	Approx. field
inner, r_i	4.19	5.32	25.6	26.4	6.11	4.96
outer, r_o	4.35	3.77	75.2	73.5	17.3	19.5

Fig. 4 also shows the sharp dependence of both the DMM and the Arrhenius-IPM life models for the treated cable on temperature, as well as the broad conservative margin between the life estimates for the full-size cable and those obtained in the laboratory for small flat specimens after [32], [33] (tested at 90 °C $\gg$ 70 °C, the rated conductor temperature of the treated cable).

The PQT for VSC HVDC extruded cables prescribed in [6] consists of 360 "24-h" cycles at dc voltage $U_{PQT} = 1.45U_0$, grouped in three periods, i.e., "true" load cycles (LC period), high load (HL) period, and zero load (ZL) period. TT load cycles are omitted both for brevity and as PQT is vital for long-term cable reliability. Since in previous investigations, the maximum field values in qualification test conditions were always found either at inner or at outer insulation [7], [8], [9], Table III quotes insulation life $L_{cycle}(r)$ in PQT conditions at inner and outer insulation of the treated cable obtained by means of the DMM model with parameters in Table I, last column, and by means of the IPM-Arrhenius model (these latter life estimates already appeared in [8]); $E(r, t)$ in block 3, Fig. 1, is calculated via the rigorous (exact) and approximate method.

As for the goal of this article, the most important comment stemming from Table III is that—as expected—PQT life from the DMM model is much greater than PQT life from the IPM-Arrhenius model (this holds also for TT life, omitted here for brevity): in particular, the ratio $R_{cycle} = L_{cycle,DMM}(r)/L_{cycle,IPM-Arr.}(r)$ ranges from 4.96 to 6.11 for inner insulation and from 17.3 to 19.5 for outer insulation, depending on whether the rigorous (exact) field or the approximate field is chosen.

The life under qualification test load cycles predicted by the DMM is higher than expected. Indeed, the approach to the selection of qualification test voltages/fields for PQT (lasting 360 days) and TT (lasting 30 days) is based on a sound experience on testing HVDC extruded cables that dates back since 2003 when the 1st Cigre TB 219 on testing such cables was issued; such approach is still the same in the current TB 852:2021 [6]. This result suggests that, while the DMM model appears as an excellent physical tool for fitting failure times at high electric fields—those used in ALTs on small specimens—it is perhaps too optimistic for the lower qualification test fields.

This might be due first of all to the fact that the DMM model has been fitted to the results of ALTs for a top-grade state-of-the-art DC XLPE compound for cables working at 90 °C, while the design temperature of the treated cable is 70 °C. Second, the higher-than-expected lives under qualification test load cycles predicted by the DMM might also be due to the fact that the DMM model postulates a massive injection and storage of charge (see hypothesis I) in Section III-A; injection and storage are surely strong at the high test fields of small-size specimens (see circles and boxes in Figs. 3 and 4) but become weaker as the electrical threshold for charge injection [27] is approached in the range of the much lower qualification test fields (30–40 kV/mm, see black and brown dashed-dotted lines in Fig. 4). As injection and storage become weaker, DMM life lines exhibit a sharp knee leading to a downward bent (see Figs. 3 and 4), whereby the dependence of life on electric field becomes much weaker; this is followed by a sudden upward curvature leading to a quick tendency to the electrical threshold, as soon as DMM life becomes totally insensitive to electric field.

Such behavior is different from the IPM and IPM-Arrhenius models in Figs. 3 and 4, which have a constant slope throughout the considered range of electric fields, from small specimen test fields to qualification test fields. Indeed, as space-charge storage and injection become less massive, the DMM aging mechanism will slow down progressively to an extent that other field-related aging processes—not directly associated with space charge—will become faster and determine HVDC cable insulation life as their time to breakdown is less than that of the DMM. Thus, they will modify the behavior of the insulation at and below the DMM threshold reducing the predicted life from infinity. In fact, the DMM uses the expression $q_c = C_q E^b$ (see hypothesis I in Section III-A) for the space charge at all fields. When the space-charge threshold is approached, this function is likely to be changed into one giving a lower amount of space charge than it predicts. According to the physics of the model, this will lead to longer lifetimes than those predicted by other aging mechanisms, which are slower than the DMM at higher fields. Therefore, considering the space-charge threshold together with the advent of other aging to breakdown mechanisms below the DMM threshold, the lifeline in this region of field can be expected to extend more in the form of a power law than is predicted by the DMM, as observed in Figs. 3 and 4. Such other aging mechanisms might be, e.g., electrochemical degradation and static Maxwell forces [17], [18], [19], omitted in the DMM model and not easy to describe accurately through physical aging and life models in general. Such processes might be responsible for the macroscopic, empirically assessed, power law dependence of life on electric field at very long lives and very low fields, which is typical of the IPM models.

Overall, both the DMM and the IPM-Arrhenius models yield much longer PQT lives than the duration of the PQT (=360 days $\approx$ 1 year). This indicates that the PQT with maximum conductor temperature set exactly to rated conductor temperature $T_{cond,max}$ might not be challenging enough, as observed in [7], [8], and [9].

As already discussed in [8], the values of PQT life L^*_{cycle} (gray-shaded cells) derived with the rigorous and the approximate field are fairly different. When the Arrhenius-IPM is

used, the rigorous field locates L^*_{cycle}—thus the most severely stressed point in the insulation—at inner insulation ($r* = r_i$), whereas the approximate field at outer insulation ($r* = r_o$). When the DMM is used, both the rigorous and the approximate field locate L^*_{cycle} at inner insulation ($r* = r_i$). It should be pointed out that the difference between PQT field with the rigorous and the approximate field is only a few percent (see [8]), but this is enough to displace the most stressed point from outer to inner insulation with the IPM-Arrhenius, which is much more sensitive to PQT field than the DMM (see above); on the contrary, with the DMM, the effect of PQT field on life is much weaker than that of temperature, and inner insulation (the hottest point) remains the most stressed with both the rigorous and approximate field.

V. Conclusion

This article has introduced the use of the DMM life model in the earlier developed procedure for life estimation of HVDC cables subjected to qualification load cycles. In this way, the life forecasts by the DMM can be compared with those from the IPM-Arrhenius life model employed to date, thereby acquiring a deeper insight into the endurance properties of such cables.

The use of the DMM model is not easy, as illustrated in this article. Indeed, first, it requires an updated set of DMM model parameters; this set has been derived here from the fitting of small specimen ALT data relevant to a state-of-the-art top-grade DC-XLPE tested under dc voltage at 90 °C. The updated parameter set has been discussed on the basis of the elemental strain theory on which the DMM relies, finding that the parameter set values are meaningful from the chemical–physical behavior viewpoint of polymeric insulation for dc cables.

Second, the updated DMM model parameter set has to be extrapolated from small specimen ALT data to the treated full-size cable to be pre-qualified according to Cigrè TB 852; this has been accomplished here having as a reference the design life of 40 years provided by the IPM-Arrhenius model. In this way, the design life agrees well with the experience on HVDC extruded cable testing and service, and the comparison DMM versus IPM-Arrhenius is consistent.

Such comparison shows that the life under qualification test load cycles predicted by the DMM is much higher than that by the IPM-Arrhenius. This might be due to the fact that the DMM model has been fitted here to the results of ALTs for a top-grade state-of-the-art DC XLPE compound for cables working at a higher design temperature than the treated cable, as well as to the fact that, as space-charge storage and injection become less massive, other slower field-related aging processes—not directly associated with space charge—might be active: e.g., electrochemical degradation and static Maxwell forces, omitted in the DMM model and not easy to be described.

Overall, both the DMM and the IPM-Arrhenius models yield much longer PQT lives than the duration of the PQT, confirming from the previous studies that the PQT with maximum conductor temperature set exactly to rated conductor temperature might not be challenging enough.

Last but not least, the small difference between PQT field with the rigorous and the approximate field calculation is enough to displace the most stressed point from outer to inner insulation with the IPM-Arrhenius, which is much more sensitive to PQT field than the DMM; on the contrary, with the DMM the effect of PQT field on life is much weaker than that of temperature, and inner insulation (the hottest point) remains the most stressed with both the rigorous and approximate field.

References

[1] J. C. Fothergill, "The coming of age of HVDC extruded power cables," in *Proc. IEEE Electr. Insul. Conf. (EIC)*, Jun. 2014, pp. 124–137.

[2] G. Mazzanti, "Issues and challenges for HVDC extruded cable systems," *Energies*, vol. 14, no. 15, pp. 1–34, 2021, doi: 10.3390/en14154504.

[3] T. Igi et al., "Qualification, installation and commissioning of world's first DC 400kV XLPE cable system," in *Proc. 10th Int. Conf. Insulated Power Cables*, Versailles, France, Jun. 2019, pp. 1–23.

[4] Y. Ohki, "News from Japan," *IEEE Elect. Insul. Mag.*, vol. 36, no. 2, pp. 50–52, Mar. 2020, doi: 10.1109/MEI.2020.9070116.

[5] G. Mazzanti and M. Marzinotto, *Extruded Cables for High Voltage Direct Current Transmission: Advance in Research and Development*. Hoboken, NJ, USA: Wiley, 2013.

[6] *Recommendations for Testing DC Extruded Cable Systems for Power Transmission at a Rated Voltage up to and Including 800 kV*, Brochure CIGRE 852, CIGRE Working Group B1.62, Paris, France, Nov. 2021.

[7] G. Mazzanti, "Life estimation of HVDC cables under the time-varying electrothermal stress associated with load cycles," *IEEE Trans. Power Del.*, vol. 30, no. 2, pp. 931–939, Apr. 2015.

[8] G. Mazzanti, "Including the calculation of transient electric field in the life estimation of HVDC cables subjected to load cycles," *IEEE Elect. Insul. Mag.*, vol. 34, no. 3, pp. 27–37, May 2018, doi: 10.1109/MEI.2018.8345358.

[9] B. Diban and G. Mazzanti, "The effect of temperature and stress coefficients of electrical conductivity on the life of HVDC extruded cable insulation subjected to type test conditions," *IEEE Trans. Dielectr. Electr. Insul.*, vol. 27, no. 4, pp. 1313–1321, Aug. 2020.

[10] G. Mazzanti, "Improved evaluation of the life lost by HVDC extruded cables due to long TOVs," *IEEE Trans. Power Del.*, vol. 37, no. 3, pp. 1906–1915, Jun. 2022.

[11] G. Mazzanti and B. Diban, "The effects of transient overvoltages on the reliability of HVDC extruded cables. Part 2: Superimposed switching impulses," *IEEE Trans. Power Del.*, vol. 36, no. 6, pp. 3795–3804, Dec. 2021.

[12] G. Mazzanti, "Updated review of the life and reliability models for HVDC cables," *IEEE Trans. Dielectr. Elect. Insul.*, vol. 30, no. 4, pp. 1371–1390, Aug. 2023, doi: 10.1109/TDEI.2023.3277415.

[13] S. Le Roy, G. Teyssèdre, and C. Laurent, "Modelling space charge in a cable geometry," *IEEE Trans. Dielectr. Electr. Insul.*, vol. 23, no. 4, pp. 2361–2367, Aug. 2016.

[14] Y. Zhan, G. Chen, and M. Hao, "Space charge modelling in HVDC extruded cable insulation," *IEEE Trans. Dielectr. Electr. Insul.*, vol. 26, no. 1, pp. 43–50, Feb. 2019.

[15] L. A. Dissado, G. Mazzanti, and G. C. Montanari, "Elemental strain and trapped space charge in thermoelectrical aging of insulating materials. Part 1: Elemental strain under thermo-electrical-mechanical stress," *IEEE Trans. Dielectr. Electr. Insul.*, vol. 8, no. 6, pp. 959–965, Dec. 2001.

[16] G. Mazzanti, G. C. Montanari, and L. A. Dissado, "Elemental strain and trapped space charge in thermoelectrical aging of insulating materials: Life modeling," *IEEE Trans. Dielectr. Electr. Insul.*, vol. 8, no. 6, pp. 966–971, Dec. 2001.

[17] J.-L. Parpal, J.-P. Crine, and C. Dang, "Electrical aging of extruded dielectric cables. A physical model," *IEEE Trans. Dielectr. Electr. Insul.*, vol. 4, no. 2, pp. 197–209, Apr. 1997.

[18] J. P. Crine, "A molecular model for the electrical aging of XLPE," in *Proc. IEEE Conf. Electr. Insul. Dielectr. Phen. (CEIDP)*, Oct. 2007, pp. 608–610.

[19] T. J. Lewis, "Polyethylene under electric stress," *IEEE Trans. Dielectr. Electr. Insul.*, vol. 9, no. 5, pp. 717–729, Oct. 2002.

[20] H. A. Alghamdi, G. Chen, and A. Vaughan, "Simulate the effect of trapped charges and trap cross-section on aging process," in *Proc. IEEE Conf. Electr. Insul. Dielectric Phenomena (CEIDP)*, Toronto, ON, Canada, Oct. 2016, pp. 27–30, doi: 10.1109/CEIDP.2016.7785678.

[21] G. Mazzanti, G. C. Montanari, and L. Simoni, "Insulation characterization in multistress conditions by accelerated life tests: An application to XLPE and EPR for high voltage cables," *IEEE Elect. Insul. Mag.*, vol. 13, no. 6, pp. 24–34, Nov/Dec. 1997.

[22] Z. Zuo, L. A. Dissado, C. Yao, N. M. Chalashkanov, S. J. Dodd, and Y. Gao, "Modeling for life estimation of HVDC cable insulation based on small-size specimens," *IEEE Elect. Insul. Mag.*, vol. 36, no. 1, pp. 19–29, Jan. 2020.

[23] C. K. Eoll, "Theory of stress distribution in insulation of high-voltage DC cables: Part I," *IEEE Trans. Electr. Insul.*, vol. EI-10, no. 1, pp. 27–35, Mar. 1975.

[24] G. C. Montanari, S. F. Bononi, M. Albertini, S. Siripurapu, and P. Seri, "The dimensional approach in the design and qualification tests of AC and DC HV cables: The Occhini approach revisited," *IEEE Trans. Power Del.*, vol. 35, no. 5, pp. 2119–2126, Oct. 2020.

[25] M. Marzinotto and G. Mazzanti, "The statistical enlargement law for HVDC cable lines—Part 1: Theory and application to the enlargement in length," *IEEE Trans. Dielectr. Electr. Insul.*, vol. 22, no. 1, pp. 192–201, Feb. 2015.

[26] G. C. Montanari and G. Mazzanti, "From thermodynamic to phenomenological multi-stress models for insulating materials without or with evidence of threshold (XLPE cables)," *J. Phys. D, Appl. Phys.*, vol. 27, no. 8, pp. 1691–1702, Aug. 1994, doi: 10.1088/0022-3727/27/8/017.

[27] L. A. Dissado, C. Laurent, G. C. Montanari, and P. H. F. Morshuis, "Demonstrating a threshold for trapped space charge accumulation in solid dielectrics under DC field," *IEEE Trans. Dielectr. Electr. Insul.*, vol. 12, no. 3, pp. 612–620, Jun. 2005.

[28] G. Mazzanti, G. C. Montanari, and L. A. Dissado, "Life modeling of AC cable insulation based on space-charge inference," in *Proc. 5th Int. Conf. Insulated Power Cables*, Versailles, France, Jun. 1999, pp. 707–712.

[29] C. Blivet, J.-F. Larché, Y. Israëli, P.-O. Bussière, and J.-L. Gardette, "Thermal oxidation of cross-linked PE and EPR used as insulation materials: Multi-scale correlation over a wide range of temperatures," *Polym. Test.*, vol. 93, Jan. 2021, Art. no. 106913.

[30] C. L. Griffiths, J. Freestone, and R. N. Hampton, "Thermoelectric aging of cable grade XLPE," in *Proc. IEEE Int. Symp. Electr. Insul.*, Arlington, VA, USA, Jun. 1998, pp. 578–582.

[31] E. S. Cooper, L. A. Dissado, and J. C. Fothergill, "Application of thermoelectric aging models to polymeric insulation in cable geometry," *IEEE Trans. Dielectr. Electr. Insul.*, vol. 12, no. 1, pp. 1–10, Feb. 2005.

[32] Y. Ohki, "Development of XLPE-insulated cable for high-voltage DC ubmarine transmission line (1) [News from Japan]," *IEEE Elect. Insul. Mag.*, vol. 29, no. 4, pp. 65–67, Jul./Aug. 2013.

[33] C. Watanabe, Y. Itou, H. Sakai, S. Katakai, M. Watanabe, and Y. Murata, "Practical application of +/-250 kV DC-XLPE cable for Hokkaido–Honshu HVDC link," Cigre Session, Paris, France, Tech. Paper B1_110, Aug. 2014.

[34] J.-P. Crine, "On the interpretation of some electrical aging and relaxation phenomena in solid dielectrics," *IEEE Trans. Dielectr. Electr. Insul.*, vol. 12, no. 6, pp. 1089–1107, Dec. 2005.

[35] M. Marzinotto and G. Mazzanti, "The practical effect of the enlargement law on the electrothermal life model for power-cable lines," *IEEE Elect. Insul. Mag.*, vol. 31, no. 2, pp. 14–22, Mar/Apr. 2015.

Giovanni Mazzanti (Fellow, IEEE) teaches HV Engineering and Power Quality at the University of Bologna, Bologna, Italy. He is a Consultant to TERNA (the Italian TSO). His research interests are reliability and diagnostics of HV insulation, power quality, renewables, and human exposure to EMF. He is the author or coauthor of more than 300 published papers and the book *Extruded Cables for HVDC Transmission: Advances in Research and Development* (Wiley-IEEE Press, 2013).

Mr. Mazzanti is a member of IEEE PES and DEIS, IEEE DEIS Technical Committee (TC) on "Smart grids," IEC TC20, CIGRÉ, CIGRE Working Group B1.91, CIGRÉ Joint Working Group B4/B1/C4.73 on "Surge and extended overvoltage testing of high voltage direct-current (HVDC) cable systems." He is the Chair of the IEEE DEIS TC on "HVDC cable systems" and responsible of the University of Bologna research team in the EU H-2020 NEWGEN project.

Open Access funding provided by 'Alma Mater Studiorum - Università di Bologna' within the CRUI CARE Agreement